

CONFIRMATION OF A RADIO-SELECTED GALAXY OVERDENSITY AT $z = 1.11$ ¹

DANIEL STERN

Jet Propulsion Laboratory, California Institute of Technology, MS 169-327, 4800 Oak Grove Drive, Pasadena, CA 91109;
 stern@zwo.fkinder.jpl.nasa.gov

BRAD HOLDEN AND S. A. STANFORD

Institute of Geophysics and Planetary Physics, Lawrence Livermore National Laboratory, L-413, Livermore, CA 94550;
 and Department of Physics, University of California, Davis, 1 Shields Avenue, Davis, CA 95616;
 bholden@igpp.ucllnl.org, adam@igpp.ucllnl.org

HYRON SPINRAD

Department of Astronomy, University of California at Berkeley, Berkeley, CA 94720; spinrad@bigz.berkeley.edu

Received 2002 July 30; accepted 2003 January 22

ABSTRACT

We report the discovery of a galaxy overdensity at $z = 1.11$ associated with the $z = 1.110$ high-redshift radio galaxy MG1 J04426+0202 (hereafter MG 0442+0202). The group, Cl 0442+0202, was found in a near-infrared survey of $z > 1$ radio galaxies undertaken to identify spatially coincident regions with a high density of objects red in $I-K'$ color, typical of $z > 1$ elliptical galaxies. Spectroscopic observations from the Keck I telescope reveal five galaxies within $35''$ of MG 0442+0202 at $1.10 < z < 1.11$. These member galaxies have broadband colors and optical spectra consistent with passively evolving elliptical galaxies formed at high redshift. Archival *ROSAT* observations reveal a 3σ detection of soft X-ray emission coincident with Cl 0442+0202 at a level 5 times greater than expected for the radio galaxy. These data suggest a rich galaxy cluster and inspired a 45 ks *Chandra X-Ray Observatory* observation. As expected, the radio galaxy is unresolved by *Chandra* but is responsible for approximately half the observed X-ray flux. The remaining *ROSAT* flux is resolved into four point sources within $15''$ of the radio galaxy, corresponding to a surface density 2 orders of magnitude higher than average for X-ray sources at these flux levels [$S(0.5-2\text{ keV}) > 5 \times 10^{-16}\text{ ergs cm}^{-2}\text{ s}^{-1}$]. One of these point sources is identified with a radio-quiet type II quasar at $z = 1.863$, akin to sources recently reported in deep *Chandra* surveys. The limit on an extended hot intracluster medium in the *Chandra* data is $S(1-6\text{ keV}) < 1.9 \times 10^{-15}\text{ ergs cm}^{-2}\text{ s}^{-1}$ (3σ , $30''$ radius aperture). Though the X-ray observations do not confirm the existence of a massive bound cluster at $z > 1$, the success of the optical/near-infrared targeting of early-type systems near the radio galaxy validates searches using radio galaxies as beacons for high-redshift large-scale structure. We interpret Cl 0442+0202 as a massive cluster in the process of formation.

Key words: cosmology: observations — galaxies: active — galaxies: evolution — galaxies: individual (MG1 J044226+0202) — X-rays

1. INTRODUCTION

The study of rich galaxy clusters at high redshift has important consequences for our understanding of structure formation in the universe and is a crucial test of cosmological models. Numerical simulations of hierarchical models such as cold dark matter predict that few massive clusters will be found at large redshift (e.g., Cen & Ostriker 1994) and that the evolution of cluster number density as a function of X-ray luminosity and temperature depends sensitively upon Ω_0 , but only weakly upon Λ and the initial power spectrum (e.g., Peebles, Daly, & Juskiewicz 1989; Evrard 1989; Eke et al. 1998). Moderate-redshift clusters from well-defined samples such as the *ROSAT* Deep Cluster Survey (RDCS; Rosati et al. 1998) have been used to constrain Ω_M and σ_8 (Borgani 2001). Distant X-ray luminous clusters provide the best lever arm for these studies. However, to date few (≈ 7) $z > 1$ clusters have been spectroscopically con-

firmed (cf. Dickinson 1995; Stanford et al. 1997; Rosati et al. 1999; Liu 2000; Rosati 2003; Thompson et al. 2001; Stanford et al. 2002).

Clusters and groups of galaxies also provide a crucial tool in the study of galaxy formation and evolution. Out to at least $z \sim 1$, clusters tend to be dominated by a population of massive elliptical galaxies that is largely homogenous and has been quiescent since at least $z \sim 1$ (e.g., Stanford, Eisenhardt, & Dickinson 1998). Finding high-redshift massive elliptical systems is difficult, but the implications for the epoch of early-type galaxy formation can be provocative, as evidenced by LBDS 53W091, a galaxy at $z = 1.55$ whose 3.5 Gyr age is comparable to the Hubble time for its redshift (Dunlop et al. 1996; Spinrad et al. 1997). An expanded census of dense environments in the early universe will provide a powerful means to test models of large-scale structure formation, characterize the galaxy populations in these environments, and study the formation epoch of early-type galaxies.

Most bound clusters beyond redshift unity have been identified from deep serendipitous X-ray surveys, from deep near-IR imaging surveys, and/or around powerful 3C radio sources. Radio galaxies are robust signposts of early collapse. In the local universe, bright radio sources are often hosted by giant elliptical and cD galaxies residing within

¹ Some of the data presented herein were obtained at the W. M. Keck Observatory, which is operated as a scientific partnership among the California Institute of Technology, the University of California, and the National Aeronautics and Space Administration. The observatory was made possible by the generous financial support of the W. M. Keck Foundation.

dense environments, and this identification has been shown to continue to higher redshift, e.g., 3C 184 at $z = 0.996$ (Deltorn et al. 1997), 3C 324 at $z = 1.21$ (Dickinson 1995), 3C 294 at $z = 1.786$ (Fabian et al. 2001), and TN J1338–1942 at $z = 4.1$ (Venemans et al. 2002). Hall et al. (2001) also show an excess population of red galaxies around radio-loud quasars at $1 \lesssim z \lesssim 2$, interpreted as being due to rich environments associated with the quasars.

In terms of studying the intracluster gas, however, clusters around the *most luminous* high-redshift radio galaxies (HzRGs) and radio-loud quasars are less than ideal, as observed X-ray emission does not necessarily derive solely from the hot gas. Hardcastle, Lawrence, & Worrall (1998) show that unresolved soft X-ray flux correlates with 5 GHz core flux for HzRGs and core-dominated radio-loud quasars. *Chandra* has also revealed soft extended X-ray emission coincident with the outer radio lobes in powerful 3C sources (e.g., Wilson, Young, & Shopbell 2000; Harris et al. 2000). This emission is thought to be due to inverse Compton scattering of cosmic microwave background photons by the relativistic plasma in radio jets or lobes. At larger redshifts, the energy density of the microwave background is higher, so that the cooling time for relativistic electrons is short. Active galactic nucleus-related soft X-ray emission should be problematic only in the youngest and most luminous radio sources at high redshift. Therefore, the next obvious step in identifying a sample of high-redshift clusters well suited to X-ray follow-up is to locate clusters identified with *less powerful* radio galaxies.

In this paper, we report the discovery of an overdensity of galaxies at $z = 1.11$ associated with the moderate-strength [$S(5 \text{ GHz}) = 110 \pm 12 \text{ mJy}$; Griffiths et al. 1995] narrow-lined HzRG MG1 J04426+0202 (hereafter MG 0442+0202). Though the X-ray observations detailed herein do not confirm a hot intracluster medium associated with this overdensity, the technique is sound and the radio galaxy clearly marks a rich location in the early universe. The group, Cl 0442+0202, was identified from a deep optical/near-IR imaging survey of radio sources at $z > 1$ selected from the 5 GHz MIT–Green Bank (MG) radio catalog (Bennett et al. 1986; Stern et al. 1999). MG 0442+0202 is a moderately steep spectrum radio source ($\alpha_{1.4\text{GHz}}^{5\text{GHz}} = -1.05$, where $S_\nu \propto \nu^\alpha$), approximately a quarter as luminous at 1.4 GHz compared with the typical $z \approx 1$ 3C HzRG. The 365 MHz morphology is double, extended by $16'' \pm 4''$ at a position angle of $-98^\circ \pm 11^\circ$ (Douglas et al. 1996). The 5 GHz morphology, measured with the VLA, reveals a triple morphology, with two nearly equal intensity lobes separated by approximately $9''$ at a position angle of 30° , flanking a centrally located core with a flux 24% of the mean lobe radio flux. Initial optical identification and redshift determination of MG 0442+0202 were obtained at Lick Observatory as part of the Berkeley effort to study MG sources (e.g., Spinrad et al. 1993; Stern et al. 1997).

We assume $H_0 = 50 \text{ h}_{50} \text{ km s}^{-1} \text{ Mpc}^{-1}$, $\Omega_M = 1$, and $\Omega_\Lambda = 0$ throughout. For this cosmology, the luminosity distance of Cl 0442+0202 is $7.88 \text{ h}_{50}^{-1} \text{ Gpc}$ and $1''$ subtends 8.58 h_{50}^{-1} proper kiloparsecs. For $H_0 = 65 \text{ km s}^{-1} \text{ Mpc}^{-1}$, $\Omega_M = 0.35$, and $\Omega_\Lambda = 0.65$, the cosmology favored by recent high-redshift supernovae and cosmic microwave background observations, these distances change very slightly: they are smaller by 0.4%. Throughout we have corrected for foreground Galactic extinction by using a

reddening of $E(B-V) = 0.155$ determined from the dust maps of Schlegel, Finkbeiner, & Davis (1998).

2. OBSERVATIONS AND RESULTS

2.1. Optical and Near-Infrared Imaging

To search for red galaxies associated with the HzRG MG 0442+0202, we obtained deep near-infrared imaging of the field by using the Gemini Twin-Arrays Infrared Camera (McLean et al. 1994) on the Lick 3 m Shane telescope. Gemini uses a dichroic beam splitter that yields two independent beams: a short-wave channel with a Rockwell NICMOS3 $256 \times 256 \text{ HgCdTe}$ array and a long-wave channel with a SBRC $256 \times 256 \text{ InSb}$ array. Gemini was used in its $0''.7 \text{ pixel}^{-1}$ mode, providing a $3' \times 3'$ field of view. Our data, obtained through J ($\lambda_c = 1.25 \mu\text{m}$; $\Delta\lambda = 0.29 \mu\text{m}$) and K' ($\lambda_c = 2.12 \mu\text{m}$; $\Delta\lambda = 0.34 \mu\text{m}$) filters for the two channels, respectively, were obtained in nonphotometric conditions on UT 1999 January 3 and December 2. The total integration time was 12 ks, and the combined K' image, reporting $2''.3$ seeing, is provided in Figure 1.

To calibrate these images, we obtained JK' snapshots of the MG 0442+0202 field on UT 1999 February 26 in photometric conditions and $0''.7$ seeing with NSFCAM (Shure et al. 1994) at the 3 m Infrared Telescope Facility (IRTF). NSFCAM was used in its $0''.3 \text{ pixel}^{-1}$ mode, providing a $77'' \times 77''$ field. Observations of standard stars from the Persson et al. (1998) list were used to calibrate the images onto the California Institute of Technology (CIT) system, defined in Elias et al. (1982). The calibrated Lick Observatory K' image reaches a depth of $K' = 20.0$ (3σ in a $4''.6$ diameter aperture).

We obtained an optical I -band ($\lambda_{\text{eff}} = 8331 \text{ \AA}$; $\Delta\lambda = 3131 \text{ \AA}$) image of MG 0442+0202 on UT 2001 January 28 with the Low Resolution Imaging Spectrometer (LRIS; Oke et al. 1995) on the Keck I telescope. This 600 s exposure, calibrated with observations of PG 1323–086 (Landolt 1992) obtained the same night, has $0''.74$ seeing and reaches a depth of 24.7 mag (3σ in $1''.5$ diameter aperture). LRIS uses a 2048×2048 back side-illuminated Tektronix CCD with $0''.212 \text{ pixel}^{-1}$, providing a $6' \times 7'.8$ field of view.

After geometrically transforming the images to a common frame, we used SExtractor (release V2.1.6; Bertin & Arnouts 1996) to create catalogs of sources selected from the K' images. Photometry was generated for $6''$ diameter apertures. Figure 2 presents resultant color-magnitude diagrams for the Lick and IRTF K' images. Compared with random extragalactic fields, the field of MG 0442+0202 has a high surface density of objects with red $I-K'$ colors. Using the IRTF infrared imaging, we find six sources in the 1.6 arcmin^2 field with $I-K' > 4$ and $K' < 20$, corresponding to a surface density of extremely red objects of 3.8 arcmin^{-2} . This is 17 times the surface density of such sources found by Barger et al. (1999) in a 61.8 arcmin^2 survey and ≈ 8 times the surface density of such sources found in the 47.2 arcmin^2 Herschel Deep Field (McCracken et al. 2000). The dotted line in Figure 2 at $I-K' \sim 4.5$ shows the red sequence characteristic of local cluster galaxies, as determined by band-shifting photometry of Coma Cluster galaxies (see Stanford et al. 1998). Particularly in the better seeing IRTF imaging where confusion is less troublesome, photometric errors less severe, and the smaller field less contaminated by field galaxies, a red sequence is evident approximately 0.5 mag

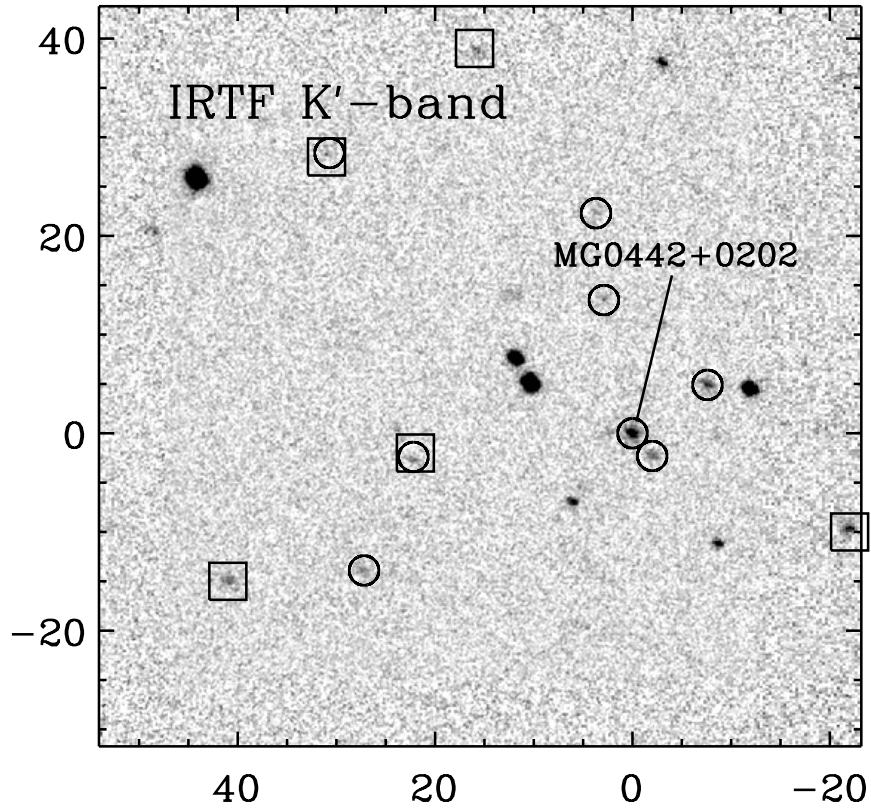
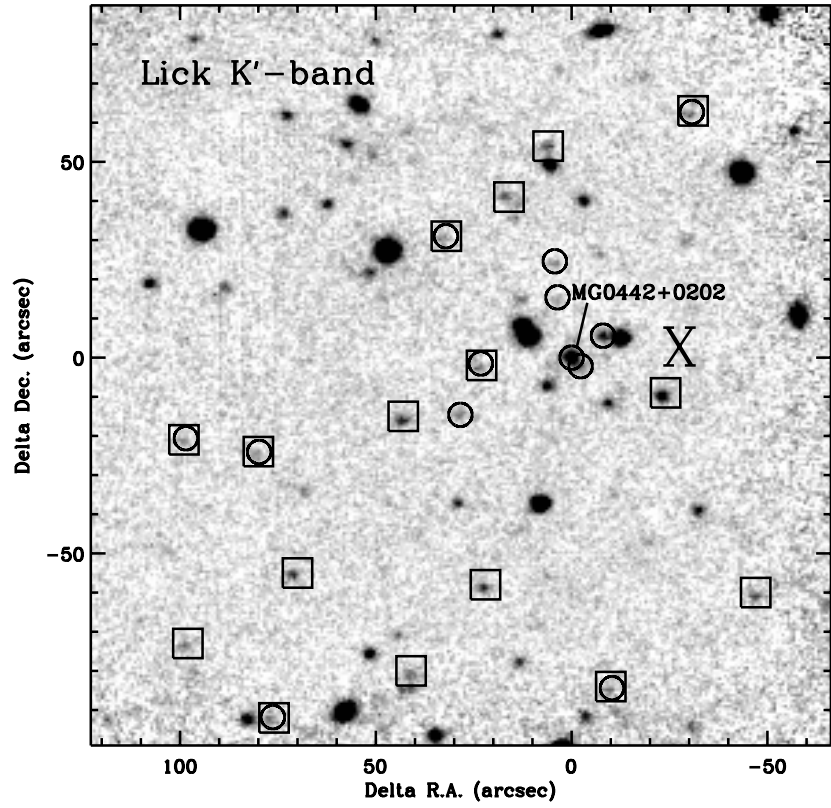


FIG. 1.—*Top*: Near-infrared Lick/Gemini K' image of the $z = 1.11$ galaxy group associated with the radio galaxy MG 0442+0202. Exposure time is 12 ks, and the image is $3\frac{1}{2}$ on a side. North is up, and east is to the left; coordinate axes provide offsets relative to MG 0442+0202, located at R.A. = $04^{\text{h}}42^{\text{m}}23^{\text{s}}.74$, decl. = $+02^{\circ}02'19''.8$ (J2000.0). *Other images*: Smaller field-of-view images from Keck/LRIS (I) and IRTF/NSFCAM (K'), $1\frac{1}{2}$ on a side. In all images, spectroscopically confirmed group members ($1.10 < z < 1.11$) are circled, sources with $I-K' > 3$ and $K' < 20$ spectroscopically shown not to reside in the group are boxed, while candidate group members, selected to have $I-K' > 3$ and $K' < 20$, are both circled and boxed. The ROSATHRI detection is marked with a large cross in the Lick image.

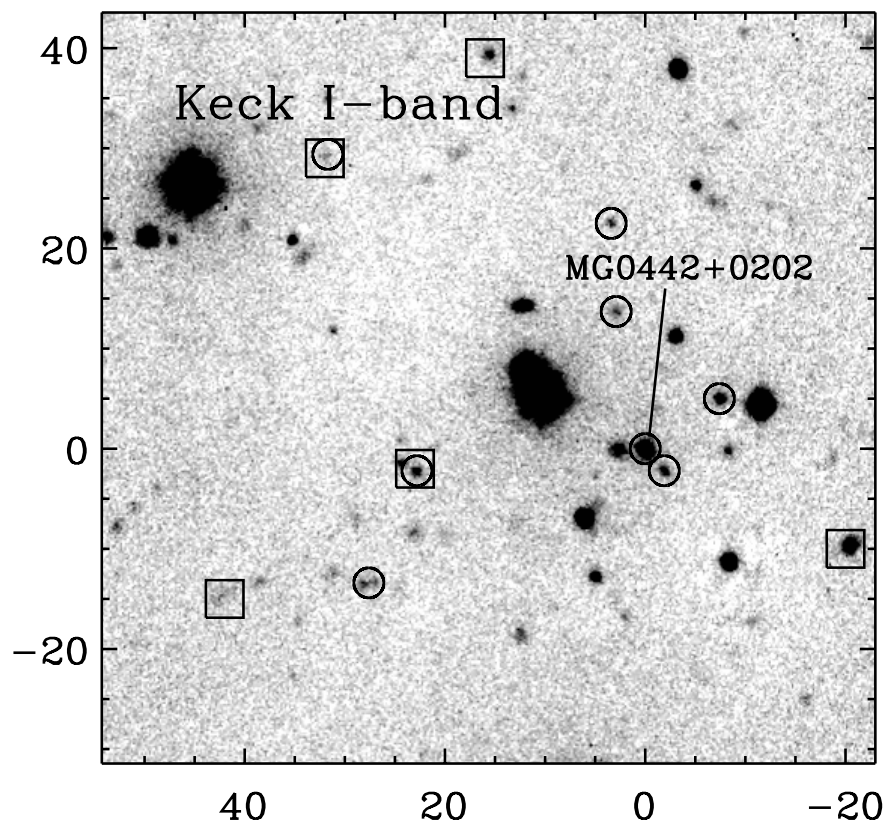


FIG. 1.—Continued

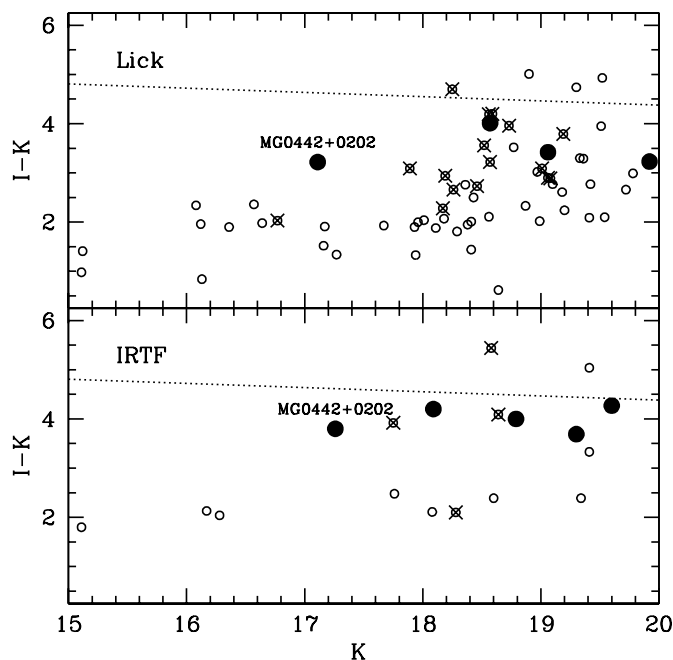


FIG. 2.—Color-magnitude diagrams for the field of MG 0442+0202. *Top*, Infrared K' image from Lick Observatory, surveying 9.9 arcmin²; *bottom*, infrared K' image from the IRTF, surveying 1.6 arcmin². Photometry was generated for 6'' diameter apertures. Galaxies spectroscopically confirmed to reside at $z \sim 1.11$ are marked with larger, filled symbols; MG 0442+0202 (labeled) is the brightest of these sources. Sources spectroscopically shown not to reside at the redshift of MG 0442+0202 are marked with crosses. The dotted line represents the no-evolution prediction for early-type galaxies based on the Coma Cluster (see text).

blueward of the no-evolution prediction. This amount of bluing in observed $I-K'$ color is consistent with the color change due to passive evolution of a single-age solar metallicity stellar population at $z = 1.11$ formed in a 0.1 Gyr burst at formation redshift $z_f = 3$ (using the updated 2000 GISSEL models of Bruzual & Charlot 1993). We targeted this red sequence for spectroscopic investigation.

2.2. Keck Spectroscopy

We obtained optical spectra of photometric candidates using LRIS in slit mask mode on the Keck I telescope. Masks on UT 2001 January 30 and UT 2001 February 19 were observed for 1.5 hr, while a fainter mask on UT 2002 February 5–6 was observed for 3.5 hr. On UT 2002 March 10 we observed a mask mainly targeting *Chandra* sources in the field for 1.5 hr. A shallow 20 minute long-slit observation of two bright *Chandra* sources was also obtained on UT 2002 March 11 during twilight. All observations used the 400 line mm⁻¹ grating ($\lambda_{\text{blaze}} = 8500$ Å; spectral resolution $\Delta\lambda_{\text{FWHM}} \approx 8$ Å) and sample the wavelength range ≈ 5000 Å to 1 μm . The 2002 March observations also implemented the blue side of LRIS, using a D560 dichroic and the 300 line mm⁻¹ grism ($\lambda_{\text{blaze}} = 5000$ Å; spectral resolution $\Delta\lambda_{\text{FWHM}} \approx 13.5$ Å), providing spectral coverage down to ≈ 3500 Å. The observations were split into 1800 s exposures with $\approx 3''$ spatial offsets performed between integrations to facilitate removal of fringing at long wavelengths. Data reductions followed standard procedures, and the spectra were flux-calibrated using observations of standard stars from Massey & Gronwall (1990). Sample optical spectra are presented in Figure 3, and results for all K' -detected

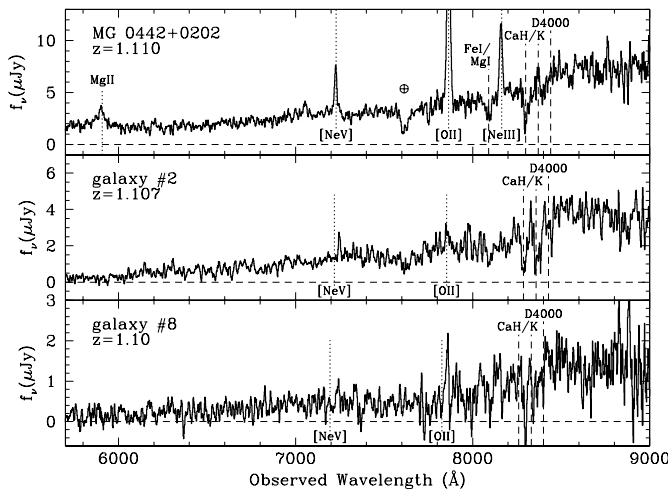


FIG. 3.—Optical spectra of three galaxies in Cl 0442+0202, obtained with the Keck I telescope. *Top*: High-redshift radio galaxy MG 0442+0202, showing several prominent narrow emission lines. Exposure times are 5.5 ks. Spectra were extracted using a $1''.5 \times 1''.5$ aperture and smoothed with a 15 Å boxcar filter. Prominent features are labeled; not all are detected. There are hints of weak [O II] in galaxy 2. The feature at 7857 Å in galaxy 8 appears to be the residual of a bright night-sky line.

sources are presented in Table 1. Redshifts were determined by visual inspection of emission and absorption features. A histogram of the redshifts we have obtained thus far in the MG 0442+0202 field is presented in Figure 4, showing a pronounced redshift spike at $z \sim 1.1$. Besides MG 0442+0202, a total of seven color-selected targets within $\lesssim 30''$ of the radio galaxy were attempted spectroscopically, of which five are confirmed cluster members and one has an inconclusive spectrum. Most of the confirmed cluster members have spectra typical of local early-type galaxies, showing strong 4000 Å breaks and weak or no emission lines. The exception is, of course, the HzRG MG 0442+0202, which shows high equivalent width, narrow, high ionization state emission features, typical of the HzRG population (e.g., McCarthy 1993).

2.3. ROSAT Archive

A search of the *ROSAT* archive reveals that High Resolution Imager (HRI; Trümper 1983) observations of the $z = 0.19$ cluster MS 0440+0204 cover Cl 0442+0202 at an off-axis angle of $13''.4$. These data, discussed in Gioia et al. (1998), were obtained in 1994 February and March and 1995 August and September. We processed the archival

TABLE 1
SUMMARY OF SPECTROSCOPIC TARGETS IN CL 0442+0202 FIELD

ID	$\Delta R.A.$ (arcsec)	$\Delta Decl.$ (arcsec)	Δr (arcsec)	I (mag)	K' (mag)	$I-K'$ (mag)	z	Notes
MG 0442+0202	20.33	17.11	3.22	1.110	Radio galaxy
Galaxy 25.....	-1.9	-2.1	2.9	22.79	18.79	4.00	1.105	Weak [O II] $\lambda 3727$
Galaxy 2	-7.6	5.2	9.2	22.58	18.57	4.01	1.107	Early type
Galaxy 29.....	3.2	13.7	14.1	23.42	21.14	2.28	1.102	Early type
Galaxy 27.....	3.9	22.7	23.0	23.15	19.92	3.23	1.100	Early type
Galaxy 8	27.4	-14.3	30.9	22.48	19.06	3.42	1.10	Early type
Quasar 37.....	-2.9	11.4	11.7	21.37	>20.0	<1.37	2.749	Quasar
Quasar 43.....	-8.8	-11.2	14.2	20.45	18.17	2.28	0.886	Quasar
Galaxy 3	-22.2	-9.5	24.1	19.98	17.89	3.09	0.939	Early type
Galaxy 104.....	24.3	-2.2	24.4	23.07	>20.0	<3.07	1.060	[O II] $\lambda 3727$
Galaxy 101.....	-14.5	-34.7	37.6	23.17	>20.0	<3.17	1.181	[O II] $\lambda 3727$
Galaxy 4	16.2	39.2	42.4	22.69	18.73	3.96	1.125	Early type
Galaxy 9	41.7	-15.8	44.6	22.95	18.25	4.70	1.02:	Early type:
Galaxy 5	6.1	51.1	51.5	22.10	19.01	3.09	1.133	Weak [O II] $\lambda 3727$
Galaxy 7	21.4	-56.6	60.5	22.75	18.56	4.19	0.94:	
Galaxy 14.....	48.7	49.6	69.5	21.96	19.06	2.90	0.658	[O II] $\lambda 3727$
Galaxy 33.....	65.3	-33.0	73.2	21.97	19.08	2.89	1.031	[O II] $\lambda 3727$
Galaxy 22.....	-45.1	-58.6	74.0	22.79	18.59	4.20	1.07:	Early type:
Galaxy 17.....	55.2	51.6	75.6	21.13	18.19	2.94	0.86:	Early type:
Galaxy 19.....	12.6	-74.8	75.8	21.19	18.46	2.73	0.62	Early type
Galaxy 16.....	-7.4	79.6	79.9	18.80	16.77	2.03	0.194	H α
Galaxy 6	67.9	-53.8	86.6	21.79	18.57	3.22	1.043	Early type
Galaxy 105.....	-62.2	-60.6	86.8	21.79	1.120	[O II] $\lambda 3727$
Galaxy 13.....	39.3	-77.9	87.3	22.08	18.52	3.56	1.261	[O II] $\lambda 3727$
Galaxy 106.....	38.8	-81.7	90.4	20.91	>20.0	<0.91	0.147	H α
Galaxy 20.....	69.7	58.7	91.1	20.92	18.26	2.66	0.693	Early type
Galaxy 102.....	-93.2	10.7	93.8	20.59	0.240	[O II] $\lambda 3727$, H α
Galaxy 103.....	-103.1	10.5	103.6	22.82	1.112	[O II] $\lambda 3727$
Galaxy 12.....	94.7	-71.8	118.8	22.98	19.19	3.79	1.269	[O II] $\lambda 3727$
Galaxy 107.....	99.7	-75.6	125.1	22.86	>20.0	<2.86	0.193	H α

NOTE.—Astrometry is relative to the radio galaxy MG 0442+0202, located at R.A. = $04^h42^m23^s.74$, decl. = $+02^\circ02'19''.8$ (J2000.0). Parameters with colons indicate uncertain measurements. Infrared photometry is from the Lick images for all sources except galaxies 25 and 29, for which the IRTF photometry is reported; the proximity of galaxy 25 to MG 0442+0202 precludes accurate photometry in the poorly seeing Lick imaging, while galaxy 29 remains undetected in the Lick imaging. Optical photometry for sources undetected in the K' images are in $3''$ diameter apertures.

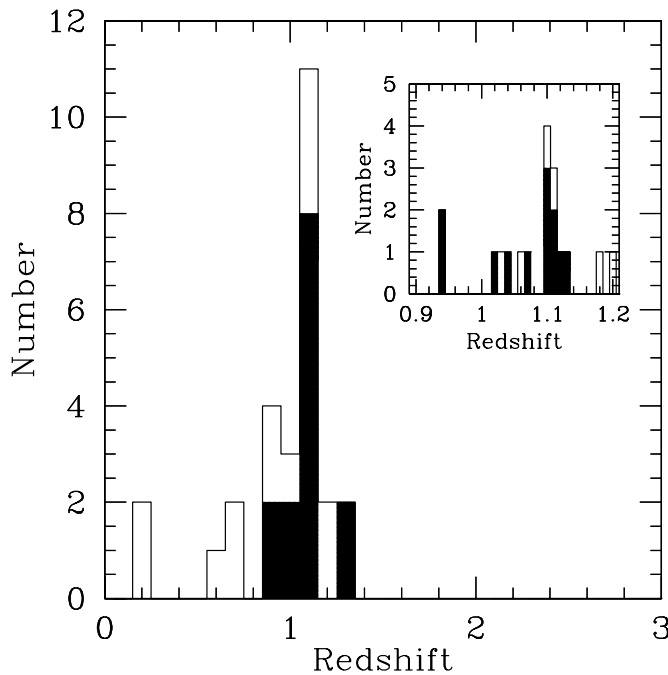


FIG. 4.—Redshift histogram of the 22 K' -detected sources in the MG 0442+0202 field for which we have spectroscopic information. Solid histogram refers to sources with $I-K' > 3$. Many of the sources with $I-K' < 3$ were observed serendipitously, fortuitously landing on the slitlet of a redder source.

data, which total 27.2 ks, and identify a 3.3σ X-ray source slightly (2σ of the point-spread function) offset from the radio galaxy. The resolution of *ROSAT* at the large off-axis angle of Cl 0442+0202 is inadequate for determining whether the X-ray emission is extended or pointlike. After correcting for the expected soft X-ray emission from the radio galaxy (Hardcastle et al. 1998), the *ROSAT* detection suggested soft X-ray emission of $\approx 10^{-13}$ ergs $\text{cm}^{-2} \text{s}^{-1}$, consistent with a high-redshift hot intracluster medium (ICM). This exciting hypothesis inspired an observation with the *Chandra X-Ray Observatory* (Weisskopf, O'Dell, & van Speybroeck 1996).

2.4. Chandra Observations

On UT 2002 February 10 we obtained a 44.1 ks observation of Cl 0442+0202 with *Chandra*. Compared with the *ROSAT* image, these data (OBS-ID 03242), taken with the Advanced CCD Imaging Spectrometer (ACIS-I), reach a greater depth with significantly improved ($\approx 0''.5$) angular resolution. We reduced and analyzed the data following standard procedures, using the *Chandra* Interactive Analysis of Observations (CIAO) software (release V2.1.2). Sources were identified independently in both soft (0.5–2 keV; S) and hard (2–7 keV; H) energy bands. Following previous analyses of deep *Chandra* data (e.g., Tozzi et al. 2001; Stern et al. 2002b), we determined a hardness ratio $(H - S)/(H + S)$, using the background-subtracted counts. A response matrix and effective area were then determined for each detected source. Assuming a Galactic $N_{\text{H}} = 9.49 \times 10^{20} \text{ cm}^{-2}$ and a typical photon index, $\Gamma = 1.4$, counts in each band were converted into fluxes. Table 2 presents the X-ray results for those *Chandra* sources contained within the optical image, along with optical magnitudes and spectroscopic redshifts, when available.

3. DISCUSSION

3.1. Chandra Results

The most striking result of the *Chandra* data is that the improved spatial resolution resolves the *ROSAT* detection into five point sources. The total soft-band flux of these sources accounts for only 20% of the *ROSAT* detection, likely due to the low significance of the *ROSAT* detection with temporal variability also possible. As expected, the radio galaxy MG 0442+0202 is detected with a relatively hard X-ray spectrum; we discuss this source further in § 3.2. At the depth of our image, $S(0.5\text{--}2 \text{ keV}) \approx 5 \times 10^{-16}$ ergs s^{-1} , *Chandra* observations of deep fields find a mean surface density of approximately 1000 sources per square degree (e.g., Stern et al. 2002b). The five sources we detect in our *Chandra* image, all within $15''$ of the HzRG, represent a surface density approximately 2 orders of magnitude higher! Unfortunately, this unusual configuration of point sources rather than an extended ICM is likely responsible for the

TABLE 2
PROPERTIES OF *Chandra* SOURCES IN Cl 0442+0202 FIELD

ID	R.A. (J2000.0)	Decl. (J2000.0)	$S_{0.5-2}^{-16}$	S_{2-10}^{-15}	$(H - S)/(H + S)$	I (mag)	z	Notes
CXO 2.....	04 42 26.90	+02 00 07.4	20.39	8.78	−0.30	23.80	...	
CXO 4.....	04 42 24.06	+02 02 14.2	5.11	11.91	0.60	23.5:	...	
CXO 5.....	04 42 23.74	+02 02 19.8	115.35	51.39	−0.29	20.91	1.110	MG 0442+0202
CXO 6.....	04 42 23.55	+02 02 31.2	17.90	3.70	−0.51	21.37	2.749	Quasar 37
CXO 7.....	04 42 23.15	+02 02 08.6	58.24	14.83	−0.55	20.42	0.886	Quasar 43
CXO 8.....	04 42 23.17	+02 02 19.8	44.75	23.08	−0.22	22.87	0.835:	Broad Mg II:
CXO 10.....	04 42 24.15	+02 03 11.0	5.91	10.11	0.37	22.49	1.133	Galaxy 5
CXO 11.....	04 42 16.36	+02 02 30.6	27.12	14.13	−0.18	22.72	...	
CXO 12.....	04 42 36.25	+02 03 25.4	20.97	13.41	−0.03	23.40	1.863	Type II quasar
CXO 16.....	04 42 34.31	+02 05 10.8	16.23	6.62	−0.35	23.24	0.772	
CXO 17.....	04 42 31.74	+02 05 08.5	36.06	16.59	−0.24	>24.7	...	
CXO 18.....	04 42 13.15	+02 04 38.5	32.98	14.78	−0.25	22.84	1.38:	Broad Mg II:

NOTES.—Units of right ascension are hours, minutes, and seconds, and units of declination are degrees, arcminutes, and arcseconds. Uncertain measurements are indicated with a colon. $S_{0.5-2}^{-16}$ is the soft-band (0.5–2 keV) flux measured in units of 10^{-16} ergs $\text{cm}^{-2} \text{s}^{-1}$. S_{2-10}^{-15} is the hard-band (2–10 keV) flux measured in units of 10^{-15} ergs $\text{cm}^{-2} \text{s}^{-1}$.

ROSAT detection. We find no diffuse emission associated with C1 0442+0202 (see § 3.4).

Of the 12 *Chandra* sources within the optical image, we have unambiguous spectroscopic redshifts for six and tentative redshifts for an additional two. Typical of follow-up of *Chandra* sources, the two sources with the softest $[(H-S)/(H+S) \approx -0.5]$ X-ray spectra are identified with luminous broad-lined quasars. Both have projected celestial positions close to C1 0442+0202 (see Table 1), but one (CXO 6) is background while the other (CXO 7) is foreground. They could provide useful probes of the environment of C1 0442+0202. The two sources with ambiguous spectra both have relatively soft X-ray spectra and optical spectra that reveal blue continua, each with the detection of a single broad emission line. We tentatively interpret both lines as Mg II $\lambda 2800$: at $z \approx 1$, the strong rest-frame UV lines characteristic of quasars have not yet entered the optical window, while the strong rest-frame optical lines have shifted to near-IR wavelengths, either beyond the optical window or at redder wavelengths where the sky is less benign.

The source CXO 10 is typical of the new population of sources being identified in deep *Chandra* images (e.g., Hornschemeier et al. 2001; Stern et al. 2002b): galaxies whose optical/near-IR properties suggest a normal galaxy with no indication of an active nucleus but are nevertheless luminous X-ray sources. Many of these sources, including CXO 10, have hard X-ray spectra, implying significant obscuration of a buried central engine. In the case of CXO 10, the optical spectrum is dominated by an old stellar population with a strong 4000 Å break. Weak [O II] $\lambda 3727$ is also present, possibly due to low levels of star formation, possibly due to the narrow-line region of the buried active nucleus.

Finally, our *Chandra* data reveal two obvious active galactic nuclei (AGNs) showing high equivalent width, high ionization state, narrow emission lines, but lacking the obvious broad-line signatures associated with quasars: CXO 5 and CXO 12. Following Seyfert nomenclature, these sources are often called *type II quasars*, and deep X-ray data have sparked a renewed interest in the population (e.g.,

Norman et al. 2002; Stern et al. 2002a; Dawson et al. 2003). The radio-loud end of this population has been studied for several decades: indeed, CXO 5 is identified with MG 0442+0202, and we discuss it in more detail in § 3.2. CXO 12 is the other type II active system identified in our data. The X-ray spectrum is relatively flat from the soft to the hard bands $[(H-S)/(H+S) = -0.03]$, providing a harder X-ray spectrum than the typical bright X-ray population. The optical spectrum (Fig. 5) shows narrow rest-frame UV emission lines with very little continuum. Stern et al. (2002a) discusses a similar source in detail (see also Norman et al. 2002; Dawson et al. 2003). Both the apparently normal galaxies and these type II quasars are being found in large numbers in surveys with the new generation of X-ray satellites. Such studies will be essential for creating an unbiased census of AGNs in the universe, thereby testing models of the X-ray background and providing a history of accretion-driven energy production in the universe.

3.2. Radio Galaxy MG 0442+0202

The $z = 1.11$ radio galaxy MG 0442+0202 is what initially drew our attention to this field. With $K' = 17.1$, MG 0442+0202 fits smoothly onto the surprisingly low-scatter Hubble, or K - z , relation of radio galaxies (e.g., see Fig. 10 in De Breuck et al. 2002). At each redshift, HzRGs are the most luminous galaxies known at observed $2 \mu\text{m}$. Since rest-frame $2 \mu\text{m}$ flux sample stellar emission from the low-mass stars that dominate the baryon content of a galaxy, this is generally interpreted as HzRGs being the most massive systems at each cosmic epoch. Indeed, our deep optical spectrum of MG 0442+0202 (Fig. 3) shows that this $z = 1.11$ radio source is hosted by an old massive galaxy. Though the dominant spectral features are strong narrow emission lines characteristic of radio galaxies (e.g., McCarthy 1993), the spectrum also clearly shows stellar light. Absorption is seen from Ca H $\lambda 3933$ and a conglomerate of Fe I/Mg I lines around 3840 Å (e.g., Pickles 1985), indicative of low-mass stars. Ca K $\lambda 3968.5$ has been filled in by [Ne III] $\lambda 3967.5$ emission. The strong 4000 Å break seen in MG 0442+0202 is another strong indicator of stellar emission in this HzRG. The break is due to the sudden onset of stellar photospheric opacity shortward of 4000 Å associated with the Fraunhofer H and K lines of Ca II, as well as various ionization stages of other elements heavier than helium (Öhman 1934).

The soft X-ray properties of core-dominated quasars are strongly correlated with their radio properties, with a radio (5 GHz) core to soft X-ray core two-point spectral index of $\alpha_X \sim 0.85$ (Worrall et al. 1994; Worrall 1997). Assuming an X-ray spectral index of $\alpha = -0.25$ (see below), the observed flux density of MG 0442+0202 at 1 keV is 3.3 nJy. For its 5 GHz radio core flux density of 12 mJy, MG 0442+0202 is slightly overluminous in the soft X-ray compared with the relation plotted by Worrall et al. (1994) for core-dominated quasars. This result is consistent with other HzRGs examined by Hardcastle et al. (1998) and may indicate non-jet-related X-ray emission originating close to the AGN.

Our *Chandra* observation detects more than 250 counts from MG 0442+0202, providing a robust hardness ratio of $(H-S)/(H+S) = -0.29$. Assuming the X-ray flux spectrum can be expressed as a simple power-law function of energy E [i.e., $F(E) \propto E^\alpha$] modified by the Galactic absorption column density in the direction of the source

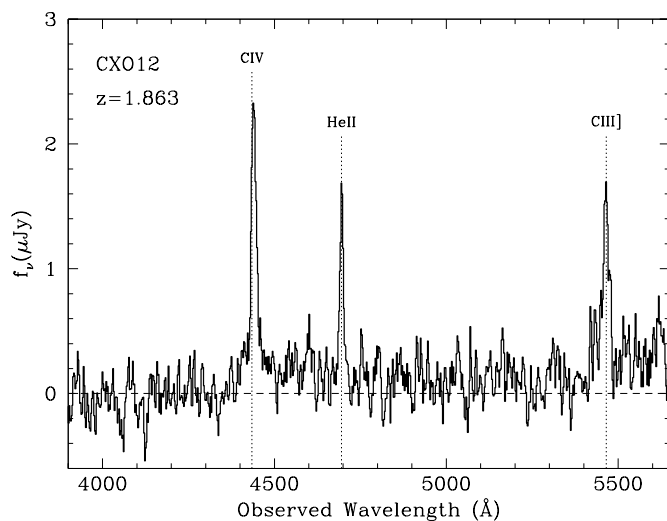


FIG. 5.—Optical spectrum of CXO 12, obtained with the Keck I telescope. Exposure time is 5.4 ks. The spectrum was extracted using a $1''.5 \times 1''.5$ aperture and smoothed with a 15 Å boxcar filter. Prominent features are labeled.

($N_H = 9.49 \times 10^{20} \text{ cm}^{-2}$), this hardness ratio corresponds to a spectral index of $\alpha \approx -0.25$, slightly flatter than the steep $\alpha \approx -0.8$ spectra commonly observed for unabsorbed AGNs (e.g., Nandra & Pounds 1994). Given the narrow-line optical-UV spectrum of the source, it is likely that MG 0442+0202 actually has an intrinsically steep X-ray spectrum that appears to be flat because of significant soft X-ray absorption by intervening material within the galaxy.

To investigate this possibility, we examined the X-ray spectrum of MG 0442+0202 more closely. Using the CIAO software, we extracted source counts within a $3''$ radius centered on MG 0442+0202; the background was determined from a rectangular region of $100''$ by $180''$. This region was chosen to overlap with the ACIS-I node in which the radio galaxy falls, node 2 for chip 3. All detected sources in this region were removed. As we were expecting a cluster in this observation, we observed with a -8 mm SIM-Z offset, hence the target did not fall on the standard aim point. We also included a $2'$ offset in the y -direction to move the potential cluster off the chip gap in the ACIS-I mosaic, which moved the target $2'$ away from the optical axis.

We binned the spectrum into 26 channels of 10 events from 0.8 to 6.0 keV, and we modeled the spectrum by using the XSPEC v11.1.2 package (Arnaud 1996) with the recently created Chartas & Getman ACIS absorption model² and using the Markevitch & Vikhlinin (2001) correction to the effective area of ACIS-I. We fitted a power law with an absorption of $9.49 \times 10^{20} \text{ cm}^{-2}$ and found the best-fitting slope for a simple power-law X-ray spectrum to be $\alpha = -0.53 \pm 0.13$. If we add an additional absorber component at the redshift of the radio galaxy and fix the intrinsic

value of $\alpha = -0.8$, we find a column density of $3.0^{+5.3}_{-3.0} \times 10^{21} \text{ cm}^{-2}$ (90% confidence limits). This model implies an unabsorbed luminosity of $2.7 \pm 0.5 \times 10^{44} \text{ ergs s}^{-1}$ (90% confidence limits; 2–10 keV), well within the quasar regime.

We also searched the extracted X-ray spectrum of MG 0442+0202 for redshifted Fe K α 6.4 keV emission, which would appear at observed 3.03 keV. Figure 6 presents the background-subtracted X-ray spectrum with a best-fit continuum model discussed above, assuming no intrinsic absorption. We find no excess emission evident at 3 keV, though we note that *Chandra's* sensitivity falls at these higher energies.

3.3. Cluster Galaxy Members

The color-selected galaxy overdensity associated with MG 0442+0202 affords us the opportunity to study early-type galaxy populations at high redshift. As seen in Figure 3, many of the galaxies associated with MG 0442+0202 have evolved stellar populations as evidenced, for example, by strong continuum decrements at 4000 Å. This feature is of particular importance as the 4000 Å decrement intensifies with the age of a stellar population, potentially providing a sensitive probe of the age of a galaxy. Most of the other $z > 1$ early-type galaxy overdensities known (see § 1) are at sufficiently high redshift ($z \gtrsim 1.25$) that this feature has shifted to challenging wavelengths for silicon-based detectors, especially from the ground, where telluric emission is severe. In such cases, astronomers are forced into the difficult situation of age-dating galaxies based on breaks at 2640 and 2900 Å, where the galaxy is several times fainter (e.g., Spinrad et al. 1997; Yi et al. 1999). The redshift of MG 0442+0202 is ideal for probing the formation history of early-type galaxies: $z = 1.11$ is sufficiently large to be cosmologically interesting, but not so large as to be challenging spectroscopically.

$D(4000) = 1.72\text{--}1.85$ for the three galaxies presented in Figure 3. By conservatively assuming that the stellar populations were formed from a single instantaneous solar metallicity burst, these galaxies have minimum ages of approximately 1 Gyr, for which we have compared the amplitudes of the $D(4000)$ break with Bruzual & Charlot (1993) stellar population synthesis models for both Salpeter (1955) and Scalo (1986) initial mass functions and a range of star formation histories (Fig. 7). The implied formation redshift is $z_f \gtrsim 1.5$. We note that several of the group members show [O II] emission at some level, suggesting some ongoing star formation. This would imply younger bluer stars diluting the $D(4000)$ amplitude, and thus an earlier formation redshift. For the exponentially decreasing star formation history plotted, the minimum age is approximately 4 Gyr, requiring formation redshifts $z_f > 5$.

We now compare the absolute magnitudes of the CL 0442+0202 galaxies with local cluster luminosity functions: for a 1 Gyr old single-burst stellar population, calculated using the Worthey (1994) models for a Salpeter (1955) initial mass function, solar metallicity, and a mass range of 0.21–10 M_\odot , the k -correction from observed K' to rest-frame Gunn i is 0.21 mag, implying $M_i = -24.9$ for MG 0442+0202 for our adopted cosmology. From a sample of 39 Abell clusters, Paolillo et al. (2001) find $M_i^* \sim -22.4$ by using the same cosmology. During the 8.8 Gyr that elapses from $z = 1.11$ to $z = 0$, our model predicts ~ 1.4 mag fading due to luminosity evolution, suggesting that MG

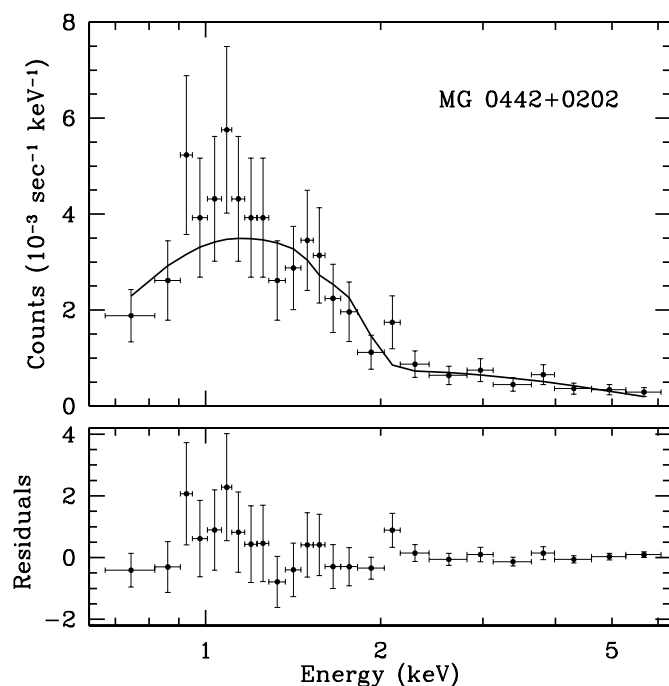


FIG. 6.—*Top*, X-ray spectrum of MG 0442+0202 with fitted spectrum folded through the detector response; *bottom*, residuals to this fit also shown, with the y -axis scale the same as in the top spectrum (units of $10^{-3} \text{ counts s}^{-1} \text{ keV}^{-1}$). Each bin contains 10 counts.

² Available at <http://www.astro.psu.edu/users/chartas/xcontdir/xcont.html>.

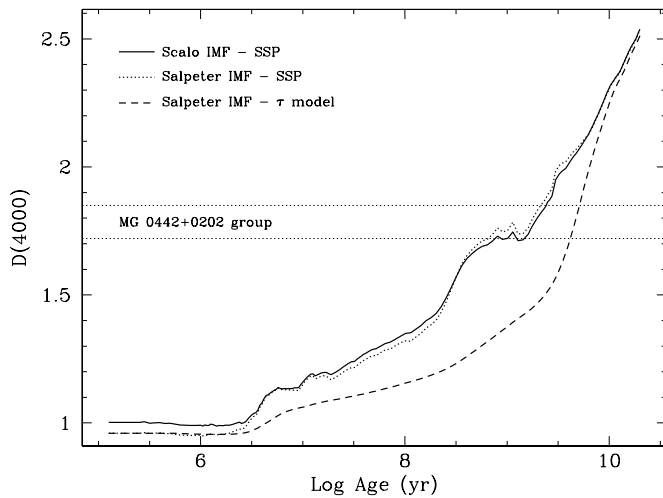


FIG. 7.—Amplitude of the D(4000) break, as defined by Hamilton (1985), for the population synthesis models of Bruzual & Charlot (1993; version BC95). All models assume solar metallicity and stellar initial mass functions within the range $0.1\text{--}125 M_{\odot}$, using either the Scalo (1986) or Salpeter (1955) parameterization. SSP refers to simple stellar populations, namely, an instantaneous burst of star formation followed by passive evolution. The τ model refers to an exponentially decreasing star formation rate with a 1 Gyr e -folding time and no gas recycling.

0442+0202 will evolve into a $\sim 3L^*$ elliptical in the present epoch if there is no additional merging. The next brightest confirmed cluster member, galaxy 2, has $M_i = -23.4$, suggesting a $\sim 0.7L^*$ elliptical galaxy in the present epoch for the same assumptions.

Including MG 0442+0202, we have identified six galaxies within an angular region of $1'$ diameter that have similar velocities. Their redshifts have a mean of 1.104. Jackknife determinations of the velocity dispersion using both the gapper method and biweights yield $\sigma \approx 600 \pm 100 \text{ km s}^{-1}$. We find similar results for the bootstrap method.

3.4. Hot Intracluster Medium?

We analyzed the *Chandra* data to study possible diffuse soft X-ray emission from a hot intracluster medium. Excluding the obvious five point sources, we implemented a simple curve-of-growth analysis. We made a series of annuli of increasing width and subtracted a background annulus from $40''$ to $60''$ in radius, all centered on MG 0442+0202. In no annulus did we achieve a 3σ detection of excess events in the 0.3 to 10.0 keV energy band. In the 1.0 to 6.0 keV band, we find a 3σ upper limit of $1.9 \times 10^{-15} \text{ ergs cm}^{-2} \text{ s}^{-1}$ for a 3 keV cluster at $z = 1.110$ within a $30''$ radius centered on the radio galaxy. This radius corresponds to $257 h_{50}^{-1} \text{ kpc}$ at the redshift of the cluster, a typical core radius for a massive cluster of galaxies. We choose 3 keV as the cluster temperature, based on the $\sim 600 \text{ km s}^{-1}$ velocity dispersion measured in § 3.3 and equation (13) in Wu, Fabian, & Fang (1999). Translating the flux limit into a luminosity, we find an upper limit of $1.5 \times 10^{43} \text{ ergs s}^{-1}$ for the bolometric luminosity of the cluster. Using the bolometric luminosity-velocity dispersion relation of equation (7) in Wu et al. 1999, we would expect a bolometric luminosity of $2.3 \times 10^{44} \text{ ergs s}^{-1}$. This would translate into a 15σ detection within the $30''$ radius, assuming a core radius of $250 h_{50}^{-1} \text{ kpc}$ and a β model with slope $\frac{2}{3}$.

4. CONCLUSIONS

Optical/near-IR imaging of the moderate-strength $z = 1.11$ radio source MG 0442+0202 has revealed an overdensity of sources with red optical to near-IR colors, typical of $z \gtrsim 1$ early-type galaxies. Spectroscopic investigations with the Keck telescope have secured redshifts for five of these galaxies in the range $z = 1.105 \pm 0.005$ within $35''$ of MG 0442+0202. These data indicate the presence of an overdensity at high redshift. The member galaxies form a homogenous population with similar colors. The colors and tightness of the color-magnitude relation support the conclusions of Stanford et al. (1998) and van Dokkum & Franx (2001), who found that the spectrophotometric properties of early-type cluster galaxies are consistent with the passive evolution of an old stellar population formed at an early cosmic epoch. Our data (Fig. 2) suggest a less steep color-magnitude relation than seen in the nearby Coma Cluster. This effect is likely due to a blue AGN contribution to the brightest galaxy in our group, MG 0442+0202. Similar flattenings of the color-magnitude relation are expected near the formation epoch of cluster elliptical galaxies, though galactic winds in single-age monolithic models can also produce such effects (e.g., van Dokkum et al. 2001).

Archival *ROSAT* data found soft X-ray emission coincident with this structure with an intensity higher than expected from the radio galaxy alone. Deeper, higher resolution *Chandra* observations reveal no extended soft X-ray emission from a hot ICM associated with the putative cluster but instead find five X-ray point sources within $15''$ of the radio galaxy, approximately 100 times the average surface density of X-ray sources at this flux level. The lack of extended X-ray emission coupled with the spectroscopically confirmed $z = 1.11$ galaxies with a tight color-magnitude relation lead us to interpret Cl 0442+0202 as a protocluster in the process of formation. Based on the sparse data presented here and the optical faintness of the associated galaxies it is difficult to fully determine the nature of the overdensity associated with MG 0442+0202. Deeper data and more extensive spectroscopy are necessary to determine whether Cl 0442+0202 will become a modest group or a rich cluster. We can safely say, however, that Cl 0442+0202 is likely a structure that has broken away from the Hubble flow but is still a long way from virialization. A weak ICM is probably already in place, with some metal enrichment from previous generations of stars, but it remains undetected since Cl 0442+0202 is not virialized and the temperature and density of the (future) ICM are far too low to produce detectable X-ray emission. As noted previously (e.g., Lubin, Oke, & Postman 2002), many optically selected clusters at $z \gtrsim 0.5$ are also underluminous in the X-ray compared with the X-ray luminosity-velocity (L_X - σ) relation for local and moderate-redshift clusters. This suggests that clusters are actively forming at these redshifts.

Accepting that Cl 0442+0202 is a cluster in the process of formation, we note that the old age of the Cl 0442+0202 member galaxies (§ 3.3) implies that the stars in clusters are older than the ICM. Similarly, based on *Hubble Space Telescope* imaging of spectroscopically confirmed members of the optically selected X-ray-underluminous cluster Cl 1324+3011 ($z = 0.76$), Lubin et al. (2002) find a high early-type fraction ($0.55^{+0.17}_{-0.14}$), indicative of a substantial tenure for these constituent galaxies. Since the ICM is processed gas, these results (1) mean the ICM is relatively young and

(2) raise the question of which galaxies are the source of the metal enrichment.

This work shows that high-redshift radio galaxies can be beacons of rich regions in the early universe, allowing the identification of clusters and protoclusters at $z \gtrsim 1$. A census of galaxy clusters at $1 \lesssim z \lesssim 1.5$ would provide a major breakthrough toward our understanding of early-type galaxy formation and cluster formation, as well as provide important constraints on basic cosmological parameters. In addition, unified models of AGNs predict that HzRGs and radio-loud quasars differ only in the orientation of their central jets relative to the observer; on average they are expected to reside in similar galactic environments. This hypothesis could be tested with a systematic study of a well-chosen sample of radio-loud galaxies and quasars.

The authors wish to recognize and acknowledge the very significant cultural role and reverence that the summit of Mauna Kea has always had within the indigenous Hawaiian community. We are most fortunate to have the

opportunity to conduct observations from this mountain. We thank Leslie Maxfield for contributions to preliminary optical observations of the radio galaxy MG 0442+0202 from Lick Observatory, and we gratefully acknowledge Charles Lawrence for enlightening discussion regarding the X-ray properties of HzRGs. We thank Megan Eckart and Fiona Harrison for Keck spectroscopy of *Chandra* sources in this field, obtained as part of the SEXSI survey (Harrison et al. 2003), and we thank Marc Davis, Alison Coil, and Ed Moran for providing the Keck *I*-band image. We are indebted to Ian McLean and Elinor Gates for building and supporting the Gemini camera at Lick Observatory, and to Kurt Adelberger for an insightful and careful referee report. Support for this project came from *Chandra* grant GO2-3194. The work of D. S. was carried out at the Jet Propulsion Laboratory, California Institute of Technology, under a contract with NASA. The work by S. A. S. and B. H. at Lawrence Livermore National Laboratory was performed under the auspices of the Department of Energy under contract W-7405-ENG-48.

REFERENCES

- Arnaud, K. A. 1996, in ASP Conf. Ser. 101, *Astronomical Data Analysis Software and Systems V*, ed. J. G. Jacoby & J. Barnes (San Francisco: ASP), 17
- Barger, A. J., Cowie, L. L., Trentham, N., Fulton, E., Hu, E. M., Songaila, A., & Hall, D. 1999, *AJ*, 117, 102
- Bennett, C. L., Lawrence, C. R., Burke, B. F., Hewitt, J. N., & Mahoney, J. 1986, *ApJS*, 61, 1
- Bertin, E., & Arnouts, S. 1996, *A&AS*, 117, 393
- Borgani, S. 2001, in *Clusters of Galaxies and the High-Redshift Universe Observed in X-Rays* (Proc. 21st Moriond Astrophysics Meeting), ed. D. M. Neumann & J. Trân Thanh Vân (Gif-sur-Yvette: Ed. Frontières)
- Bruzual A., G., & Charlot, S. 1993, *ApJ*, 405, 538
- Cen, R., & Ostriker, J. P. 1994, *ApJ*, 429, 4
- Dawson, S., McCrady, N., Stern, D., Eckart, M. E., Spinrad, H., Liu, M. C., & Graham, J. R. 2003, in preparation
- De Breuck, C., van Breugel, W., Stanford, S. A., Röttgering, H., Miley, G., & Stern, D. 2002, *AJ*, 123, 637
- Deltorn, J.-M., Le Fèvre, O., Crampton, D., & Dickinson, M. 1997, *ApJ*, 483, L21
- Dickinson, M. 1995, in ASP Conf. Ser. 86, *Fresh Views of Elliptical Galaxies*, ed. A. Buzzoni, A. Renzini, & A. Serrano (San Francisco: ASP), 283
- Douglas, J. N., Bash, F. N., Bozyan, F. A., Torrence, G. W., & Wolfe, C. 1996, *AJ*, 111, 1945
- Dunlop, J. S., Peacock, J. A., Spinrad, H., Dey, A., Jimenez, R., Stern, D., & Windhorst, R. A. 1996, *Nature*, 381, 581
- Eke, V. R., Cole, S., Frenk, C. S., & Patrick, H. J. 1998, *MNRAS*, 298, 1145
- Elias, J. H., Frogel, J. A., Matthews, K., & Neugebauer, G. 1982, *AJ*, 87, 1029
- Evrard, A. 1989, *ApJ*, 341, L71
- Fabian, A. C., Crawford, C. S., Ettori, S., & Sanders, J. S. 2001, *MNRAS*, 322, L11
- Gioia, I. M., Shaya, E. J., Le Fèvre, O., Falco, E. E., Falco, G. A., & Hammer, F. 1998, *ApJ*, 497, 573
- Griffiths, M., Wright, M., Burke, B., & Ekers, R. 1995, *ApJS*, 97, 347
- Hall, P. B., et al. 2001, *AJ*, 121, 1840
- Hamilton, D. 1985, *ApJ*, 297, 371
- Hardcastle, M. J., Lawrence, C. R., & Worrall, D. M. 1998, *ApJ*, 504, 743
- Harris, D. E., et al. 2000, *ApJ*, 530, L81
- Harrison, F. A., Eckart, M. E., Mao, P., Helfand, D., & Stern, D. 2003, *ApJ*, submitted
- Hornschemeier, A. E., et al. 2001, *ApJ*, 554, 742
- Landolt, A. U. 1992, *AJ*, 104, 340
- Liu, M. C., Dey, A., Graham, J. R., Bundy, K. A., Steidel, C. C., Adelberger, K., & Dickinson, M. E. 2000, *AJ*, 119, 2556
- Lubin, L. M., Oke, J. B., & Postman, M. 2002, *AJ*, 124, 1905
- Markevitch, M., & Vikhlinin, A. 2001, *ApJ*, 563, 95
- Massey, P., & Gronwall, C. 1990, *ApJ*, 358, 344
- McCarthy, P. J. 1993, *ARA&A*, 31, 639
- McCracken, H. J., Metcalfe, N., Shanks, T., Campos, A., Gardner, J. P., & Fong, R. 2000, *MNRAS*, 311, 707
- McLean, I. S., et al. 1994, *Proc. SPIE*, 2198, 457
- Nandra, K., & Pounds, K. A. 1994, *MNRAS*, 268, 405
- Norman, C., et al. 2002, *ApJ*, 571, 218
- Öhman, Y. 1934, *ApJ*, 80, 171
- Oke, J. B., et al. 1995, *PASP*, 107, 375
- Paolillo, M., Andreon, S., Longo, G., Puddu, E., Gal, R. R., Scaramella, R., Djorgovski, S. G., & de Carvalho, R. 2001, *A&A*, 367, 59
- Peebles, P. J. E., Daly, R. A., & Juszkievicz, R. 1989, *ApJ*, 347, 563
- Persson, S. E., Murphy, D. C., Krzeminski, W., Roth, M., & Rieke, M. J. 1998, *AJ*, 116, 2475
- Pickles, A. J. 1985, *ApJS*, 59, 33
- Rosati, P. 2003, in *Wide Field Surveys in Cosmology*, ed. Y. Mellier & S. Colombi (Gif-sur-Yvette: Ed. Frontières), in press
- Rosati, P., della Ceca, R., Norman, C., & Giacconi, R. 1998, *ApJ*, 492, L21
- Rosati, P., Stanford, S. A., Eisenhardt, P. R., Elston, R., Spinrad, H., Stern, D., & Dey, A. 1999, *AJ*, 118, 76
- Salpeter, E. E. 1955, *ApJ*, 121, 161
- Scalo, J. M. 1986, *Fundam. Cosmic Phys.*, 11, 1
- Schlegel, D., Finkbeiner, D., & Davis, M. 1998, *ApJ*, 500, 525
- Shure, M. A., Toomey, D. W., Rayner, J. T., Onaka, P. M., & Denault, A. J. 1994, *Proc. SPIE*, 2198, 614
- Spinrad, H., Dey, A., Stern, D., Peacock, J. A., Dunlop, J., Jimenez, R., & Windhorst, R. A. 1997, *ApJ*, 484, 581
- Spinrad, H., Dickinson, M., Schlegel, D., & González, R. 1993, in ASP Conf. Ser. 51, *Observational Cosmology*, ed. G. Chincarini, A. Iovino, & D. Maccagni (San Francisco: ASP), 585
- Stanford, S. A., Eisenhardt, P. R. M., & Dickinson, M. 1998, *ApJ*, 492, 461
- Stanford, S. A., Elston, R., Eisenhardt, P. R. M., Spinrad, H., Stern, D., & Dey, A. 1997, *AJ*, 114, 2232
- Stanford, S. A., Holden, B., Rosati, P., Eisenhardt, P. R. M., Stern, D., Squires, G., & Spinrad, H. 2002, *AJ*, 123, 619
- Stern, D., Dey, A., Spinrad, H., Maxfield, L. M., Dickinson, M. E., Schlegel, D., & González, R. A. 1999, *AJ*, 117, 1122
- Stern, D., et al. 2002a, *ApJ*, 568, 71
- Stern, D., Spinrad, H., Dey, A., Dickinson, M., & Schlegel, D. 1997, in *The Hubble Space Telescope and the High-Redshift Universe*, ed. N. Tanvir, A. Aragón-Salamanca, & J. Wall (Singapore: World Scientific), 413
- Stern, D., et al. 2002b, *AJ*, 123, 2223
- Thompson, D., et al. 2001, *A&A*, 377, 778
- Tozzi, P., et al. 2001, *ApJ*, 562, 42
- Trümper, J. 1983, *Adv. Space Res.*, 2, 142
- van Dokkum, P. G., & Franx, M. 2001, *ApJ*, 553, 90
- van Dokkum, P. G., Stanford, S. A., Holden, B. P., Eisenhardt, P. R., Dickinson, M., & Elston, R. 2001, *ApJ*, 552, L101
- Venemans, B. P., et al. 2002, *ApJ*, 569, 11
- Weisskopf, M. C., O'Dell, S. L., & van Speybroeck, L. P. 1996, *Proc. SPIE*, 2805, 2
- Wilson, A. A., Young, A. J., & Shopbell, P. L. 2000, *ApJ*, 544, L27
- Worrall, D. M. 1997, in *Relativistic Jets in AGNs*, ed. M. Ostrowski, M. Sikora, G. Madejski, & M. Begelman (Krakow: Astron. Obs. Jagiellonian Univ.), 20
- Worrall, D. M., Lawrence, C. R., Pearson, T. J., & Readhead, A. C. S. 1994, *ApJ*, 420, L17
- Worthey, G. 1994, *ApJS*, 95, 107
- Wu, X.-P., Xue, Y.-J., & Fang, L.-Z. 1999, *ApJ*, 524, 22
- Yi, S., Lee, Y. W., Woo, J. H., Park, J. H., Demarque, P., & Oemler, A. J. 1999, *ApJ*, 513, 128